Quantitative Proteomics Identifies Conserved Proteins and Altered Regulation of Mucin-16 in Low Grade Serous Ovarian Cancers

Christopher M. Tarney[1,2*], Paulette Mhawech-Fauceglia[1], Jonathan D. Ogata[1,3], Julie Oliver[1,3], Tamara Abulez[1,3], Philip A. Branton[4], Saeid Movahedi-Lankarani[5], Brian L. Hood[1,3], Kelly A. Conrads[1,3], Kendal Rosalik[6], Kwong-Kwok Wong[7], David M. Gershenson[7], Sanghoon Lee[7], Anil K. Sood[7], Robert C. Bast, Jr[8], Kathleen M. Darcy[1-3], Neil T. Phippen[1,2], G. Larry Maxwell[1,2,9], Thomas P. Conrads[1,2,9], Nicholas W. Bateman[1-3*]

[1]Gynecologic Cancer Center of Excellence, Department of Gynecologic Surgery and Obstetrics, Uniformed Services University and Walter Reed National Military Medical Center, Bethesda, MD 20889, USA.

[2]The John P. Murtha Cancer Center, Uniformed Services University and Walter Reed National Military Medical Center, MD 20889, USA

[3]Henry M. Jackson Foundation for the Advancement of Military Medicine, Inc. Bethesda, MD 20817, USA.

[4]Joint Pathology Center. Silver Spring, MD 20910 USA.

[5]Department of Pathology and Laboratory Medicine, Inova Health System, VA 22003, USA.

[6]Department of Gynecologic Surgery and Obstetrics, Madigan Army Medical Center, Joint Base Lewis-McChord, WA 98431, USA.

[7]Department of Gynecologic Oncology and Reproductive Medicine, The University of Texas MD Anderson Cancer Center, Houston, TX 77030, USA.

[8]Department of Experimental Therapeutics, The University of Texas MD Anderson Cancer Center, Houston, TX 77030, USA

[9]Women's Health Integrated Research Center, Women's Service Line, Inova Health System, VA 22003, USA.

*Authors contributed equally

Keywords: high-grade serous ovarian cancer, low-grade serous ovarian cancer, HGSOC, LGSOC, 5'-nucleotidase, NT5E, cluster of differentiation 73, CD73, mucin-16, MUC16, cancer antigen 125, CA125, quantitative proteomics

Address correspondence to: Nicholas W. Bateman, email: batemann@whirc.org or Thomas P. Conrads, email: conrads@whirc.org, 3289 Woodburn Rd, Suite 375, Annandale, VA 22003; Tel: 703-207-3357; Fax: 703-560-0919.

Abstract

Background: Low-grade serous ovarian carcinoma (LGSOC) is a rare and largely chemoresistant subtype of epithelial ovarian cancer. Unlike treatment for high-grade serous ovarian cancer (HGSOC), management options for LGSOC patients are limited, in part, due to a lack of deep molecular characterization of this disease. To address this limitation, we aimed to define highly conserved proteome alterations in LGSOC by performing deep quantitative proteomic analysis of tumors collected from LGSOC (n=12) and HGSOC (n=24) patients or normal fallopian tube tissues (n=12) and validating proteins within two independent proteomic datasets of LGSOC (n=25) and HGSOC (n=49) tumors.

Results: Our efforts identified 275 protein alterations conserved between LGSOC and HGSOC tumors that exhibit high quantitative correlation between discovery and validation cohorts (Spearman Rho ≥ 0.82, $P < 1E-4$). Conserved proteins elevated in LGSOC tumors were enriched for pathways regulating cell adhesion and defective cellular apoptosis signaling and candidates mapping as putative drug targets included 5'-nucleotidase/ cluster of differentiation 73 (NT5E/CD73). We also identified MUC16 (CA125) as significantly elevated in LGSOC versus HGSOC tumors and confirmed this by immunohistochemistry analysis between three independent reviewers. We also find that MUC16 exhibits a more apical versus membrane-staining pattern in LGSOC tumors, suggesting unique regulation of MUC16 in this disease subtype.

Conclusion: Our efforts define highly conserved protein alterations distinguishing LGSOC from HGSOC tumors, including CD73, as well as the novel identification that MUC16 is elevated and exhibits more apical staining pattern in LGSOC tumor tissues. These findings deepen our molecular understanding of LGSOC and provide unique insights into highly conserved proteome alterations in LGSOC tumors.

61 **Introduction**

62 Despite overall improvements in mortality, ovarian cancer is one of the most lethal
63 gynecologic malignancies with fewer than half of women surviving five years beyond initial
64 diagnosis[1]. In 2024, the American Cancer Society estimates that 19,680 women will be diagnosed
65 with ovarian cancer and 12,740 (64%) will die from their disease[2]. Epithelial ovarian cancer is the
66 most common histologic subtype of ovarian cancer and includes high-grade serous, low-grade
67 serous, mucinous, clear cell, endometrioid, and carcinosarcoma. High-grade serous ovarian cancer
68 (HGSOC) is the most common histologic subtype and is treated with a combination of
69 cytoreductive surgery and platinum-taxane chemotherapy. Low-grade serous ovarian cancer
70 (LGSOC) is responsible for 2-5% of ovarian cancer and is an overall challenging disease to treat
71 given the high rate of chemoresistance of this disease compared to HGSOC[3].

72 Historically, the hypothesis was that LGSOC ultimately progressed to HGSOC, but current
73 opinion suggests these two disease processes areindependent[4]. From a molecular standpoint, both
74 HGSOC and LGSOC vary by morphology and somatic mutations. HGSOC is associated with
75 TP53 mutations while LGSOC often harbors mutations in Kirsten rat sarcoma virus (KRAS), the
76 proto-oncogene B-Raf (BRAF), receptor tyrosine-protein kinase erbB-2 (ERBB2), beta-catenin
77 (CTNNB1), and phosphatidylinositol 4,5-bisphosphate 3-kinase catalytic subunit alpha isoform
78 (PIK3CA)[4]. However, co-existing high-grade and low-grade tumors often exhibit the same
79 mutation and lack a TP53 mutation, suggesting there may be a stepwise, non-TP53 related
80 pathogenic process[4]. More importantly, an understanding of genomic differences between these
81 disease subtypes has also introduced new treatments for LGSOC patients [5].

82 Although the proteomic characterization of HGSOC is more widely described, there is
83 currently limited proteomic data characterizing LGSOC tumors[6,7]. Some hypotheses suggest that

LGSOC and HGSOC may originate from fallopian tube epithelium[3,8], which provides a rationale for its incorporation in the proteomic evaluation of these tumors. As a result, we sought to perform a deep proteomic investigation evaluating tumors from patients diagnosed with LGSOC and HGSOC as well as normal fallopian tube tissues from women with benign disease to better understand the differences in molecular alterations between these tumors. We further aimed to define highly conserved proteome alterations between LGSOC and HGSOC tumors by integrating our discovery findings with previously described proteomic analyses of these tumor types[6,7,9].

107 **Methods**

108 **Patient cohort and tissue collections**

109 Formalin-fixed, paraffin-embedded (FFPE) LGSOC and HGSOC tumor and normal fallopian tube
110 tissues were obtained from Inova Fairfax Hospital (Falls Church, VA) under a less than minimal-
111 risk WCG IRB-approved protocol #20122048 with waivers for consent and HIPAA authorization
112 and evaluated under protocol #14-1679 with an exempt determination by the WCG IRB in
113 accordance with the use of de-identified data under US Federal regulation 45 CFR 46.102(f).
114 Benign fallopian tube tissues (FT) (n=12), as well as tumor tissues from LGSOC (n=12) and
115 HGSOC (n=24) patients, were sectioned onto 8 µm polyethylene naphthalate membrane slides and
116 hematoxylin-eosin stained. Equivalent areas of whole tissue from FT and tumor epithelium were
117 collected using laser microdissection, avoiding areas of necrosis and hemorrhage, directly into 50
118 µL of Optima™ LC/MS Grade water (Fisher Chemical) in microcentrifuge tubes and stored at -
119 80ºC until sample preparation.

120

121 **Sample preparation for quantitative proteomic analysis**

122 Protein from FFPE tissues was prepared for quantitative mass spectrometry (MS)-based
123 proteomics as previously described[10]. Briefly, tissues were transferred to MicroTubes (Pressure
124 BioSciences, Inc., Easton, MA, USA) including 20 µL of 100 mM TEAB (pH 8.0)/10%
125 acetonitrile and underwent pressure-assisted trypsin digestion employing a barocycler (2320EXT,
126 Pressure BioSciences, Inc.) and a heat-stable form of trypsin (SMART Trypsin, Thermo Fisher
127 Scientific, Inc., Waltham, MA, USA). Peptide digest concentrations were determined using the
128 bicinchoninic acid assay (BCA; Thermo Fisher Scientific, Inc.). Peptides were labeled with
129 isobaric tandem mass tag (TMT) reagents according to the manufacturer's instructions (TMT11™

130 Isobaric Label Reagent Set, Thermo Fisher Scientific). Sample multiplexes were reversed-phase
131 fractionated (basic pH) on a 1260 Infinity II offline liquid chromatography system (Agilent
132 Technologies, Inc., Santa Clara, CA, USA) into 96 fractions using a linear gradient of acetonitrile
133 (0.69% min^{-1}) followed by concatenation into 24 pooled fractions. Pooled fractions were
134 lyophilized in a Speed-Vac and stored at -20 ºC until resuspended in 25 mM NH_4HCO_3 and
135 analyzed by liquid chromatography-tandem mass spectrometry (LC-MS/MS).
136
137 **LC-MS/MS Analysis**
138 Peptide identifications and quantitation for TMT multiplexes were performed as recently
139 described[9]. Liquid chromatography-tandem mass spectrometry (LC-MS/MS) analyses of TMT11
140 multiplexes were performed on a nanoflow high-performance LC system (EASY-nLC 1200,
141 Thermo Fisher Scientific, Inc.) coupled online with an Orbitrap mass spectrometer (Q Exactive
142 HF-X, Thermo Fisher Scientific, Inc.). Samples were loaded on a reversed-phase trap column
143 (Acclaim™ PepMap™ 100 Å, C-18, 20 mm length, nanoViper Trap column, Thermo Fisher
144 Scientific, Inc.) and eluted on a heated (50 °C) reversed-phase analytical column (Acclaim™
145 PepMap™ RSLC C-18, 2 µm, 100 Å, 75 µm × 500 mm, nanoViper, Thermo Fisher Scientific,
146 Inc.) by developing a linear gradient from 2% mobile phase A (2% acetonitrile, 0.1% formic acid)
147 to 32% mobile phase B (95% acetonitrile, 0.1% formic acid) over 120 min at a constant flow rate
148 of 250 nL/min. Full scan mass spectra (MS) were acquired using a mass range of *m/z* 400-1600,
149 followed by selection of the top 12 most intense molecular ions in each MS scan for high-energy
150 collisional dissociation (HCD). Instrument parameters were as follows: Full MS: AGC, 3 × 10e6;
151 resolution, 60 k; S-Lens RF, 40%; max IT, 45 ms; MS2: AGC, 10e5; resolution, 45 k; max IT, 95
152 ms; quadrupole isolation, 1.0 *m/z*; isolation offset, 0.2 *m/z*; NCE, 34; fixed first mass, 100 *m/z*;

153 intensity threshold, 2 × 10e5; charge state, 2–4; dynamic exclusion, 20 s with 10 ppm tolerance,
154 TMT optimization. Global protein-level abundances were generated from peptide spectral matches
155 identified by searching .raw data files against a publicly available, non-redundant human proteome
156 database (http://www.uniprot.org/, SwissProt, Homo sapiens, downloaded 12-01-2017 using
157 Mascot (Matrix Science, v2.6.0), Proteome Discoverer (v2.2.0.388, Thermo Fisher Scientific,
158 Inc.), and in-house tools using identical parameters as previously described[9].
159

160 **Bioinformatic Analysis**

161 Differential analyses of TMT-11 data matrixes were performed using the LIMMA package
162 (version 3.8)[11] in R (version 3.6) and Mann-Whitney U rank sum testing in MedCalc (version
163 19.0.3). Pathway analysis was performed using MSigDB and GSEA[12] considering hallmark and
164 canonical pathways using default enrichment settings, i.e. significantly enriched pathways
165 satisfied a false discovery rate < 0.05 or STRING (https://string-db.org/) using default parameters
166 for Homo Sapiens. Visualizations were generated using SRplot[13] , GraphPad Prism (v.10.0.3), or
167 MedCalc. Global proteome data for LGSOC and HGSOC validation cohorts were previously
168 reported[6,7,9] and HGSOC data[9] prioritized for this analysis was focused on tumors where tissue
169 source site was designated as primary.
170

171 **Immunohistochemical analysis of mucin-16 (MUC16)/ cancer antigen 125 (CA125)**

172 LGSOC and HGSOC tissues were sectioned onto charged glass slides, fixed with 100% methanol,
173 incubated at 5 min at ambient temperature then rinsed with phosphate-buffered saline (PBS).
174 Tissue was permeabilized by incubating with 0.05% triton-PBS for 15 min and 2.5% normal goat
175 serum. The slides were incubated overnight at 4 °C with anti-CA125 mouse monoclonal antibody

176 (Clone M11, Agilent Dako, Santa Clara, CA, USA 1:1000). Dako's Envision diaminobenzidine
177 (DAB) detection system was used to label bound antibody complexes. Normal lung tissue was
178 used as the positive tissue control. Following detection, slides were counterstained with
179 hematoxylin then dehydrated and cover slipped. Stained tissue sections were scanned on an Aperio
180 ScanScope XT slide scanner (Leica Microsystems, Wetzlar, Germany). Digital images underwent
181 expert pathology review (P.M.F., P.A.B., S.M.L.) and a Cohen's kappa statistic was calculated to
182 assess inter-rater variability of MUC16-positive tumor cell reviews categorized as quintiles using
183 the irr package (version 0.84.1). Odds ratio analysis was performed by comparing tumors classified
184 as exhibiting a "Apical" or "Apical/ Membranous" staining pattern designations by expert
185 pathology review using MedCalc (version 20.109).
186
187
188
189
190
191
192
193
194
195
196
197
198

199 **Results**

200 **Quantitative proteomic analyses of whole tissue collections from normal fallopian tube as**
201 **well as low and high-grade serous ovarian cancers.**

202 We performed multiplexed, quantitative proteomic analyses of whole tissue equivalents collected
203 from low-grade (LGSOC, n=12) or high-grade serous ovarian cancer (HGSOC, n=24) tumors and
204 fallopian tube tissues (FT, n=12) from women with benign disease (Figure 1, Table 1,
205 Supplementary Table 1). Global proteomic analyses resulted in the quantitation of 7,043 proteins
206 across all patient samples (Supplementary Table 2). Principal component analysis of top variably
207 abundant proteins quantified across all patient samples explained 37.1% (PC1) and 8.9% (PC2) of
208 the variance between FT, LGSOC, and HGSOC tissue collections (Figure 2A). Differential
209 analysis of proteins quantified between HGSOC or LGSOC and FT collections identified both co-
210 altered as well as unique protein alterations between these comparisons (Figure 2B, Supplementary
211 Table 3 and 4).

212 Pathway analysis of co-altered proteins elevated in HGSOC and LGSOC compared to FT
213 identified enrichment of top pathways correlating with regulation of protein translation (i.e., 40S/
214 60S ribosome and eukaryotic translation elongation) as well as protein metabolism (i.e., response
215 of EIF2AK4 to amino acid deficiency and selenoamino acid metabolism) in tumor samples (Figure
216 2C, Supplementary Table 5). Pathways enriched among proteins elevated in FT tissues largely
217 correlated with regulation of cilium development as well as organelle biogenesis Figure 2C,
218 Supplementary Table 5). Proteins uniquely elevated in HGSOC vs FT identified pathways largely
219 associated with cell cycle regulation while those enriched for proteins uniquely elevated in LGSOC
220 vs FT correlated with pathways regulating epithelial to mesenchymal transition and hematopoietic
221 cell-related signaling (Figure 2D, Supplementary Table 6).

222 **Characterization and validation of proteome alterations between low and high-grade serous**
223 **ovarian cancers**

224 Our discovery cohort of LGSOC and HGSOC tumors was compared with global proteome data of
225 tumor tissues collected from two independent cohorts of women diagnosed with LGSOC[6,7] (n=25)
226 or HGSOC[7,9] (n=49) (Figure 3A). Differential analysis of proteins quantified in LGSOC and
227 HGSOC tumors identified 785 proteins as significantly altered between these tumor types (Figure
228 3B). Top protein alterations included proliferation marker protein Ki-67 (MKI67) elevated in
229 HGSOC and multiple collagen isoforms in LGSOC tumors (Figure 3B, Supplementary Table 7).
230 Comparison of these protein alterations across discovery and validation cohorts identified 275
231 significantly co-altered proteins between these disease subtypes that further exhibit high
232 quantitative correlation (Figure 3C) with two proteins, dihydropyrimidine dehydrogenase
233 [NADP(+)] (DPYD) and Fructose-1,6-bisphosphatase 1 (FBP1), exhibiting discordant abundance
234 between cohorts (Supplementary Table 8). Pathway analysis of these features showed proteins
235 elevated in LGSOC tumors were enriched for pathways regulating intercellular adhesion and
236 defective cellular apoptosis signaling while proteins elevated in HGSOC tumors showed
237 enrichment of pathways largely regulating DNA replication and cell cycle (Figure 3D3D,
238 Supplementary Table 9). We further investigated proteins that are putative drug targets in LGSOC
239 and HGSOC tumors and identified 27 features (Supplementary Table 8). Putative drug targets
240 exhibiting the largest abundance differences between these tumor types included Annexin A1
241 (ANXA1) and 5'-nucleotidase/ cluster of differentiation 73 (NT5E/CD73) as elevated in LGSOC
242 tumors and DNA topoisomerase 2-alpha (TOP2A) as well as cyclin-dependent kinase 1 (CDK1)
243 as elevated in HGSOC tumors.

244 We also identified mucin-16 (MUC-16), also known as cancer antigen 125 (CA125), as
245 significantly elevated in LGSOC versus HGSOC tumors passing false-discovery rate (FDR) < 0.05
246 expectations in discovery and validation A cohorts (Figure 4A) and exhibiting concordant
247 abundance in validation B cohort as elevated in LGSOC versus HGSOC tumors with an FDR =
248 0.052. Circulating MUC16/CA125 levels are assessed as part of routine diagnosis and disease
249 monitoring in the clinical management of ovarian cancer[3,8]. To uncover whether other putatively
250 conserved protein candidates elevated in LGSOC tumors are predicted to interact with MUC16,
251 we investigated highly conserved protein alterations using the STRING protein interaction
252 network (string-db.org) and identified nesprin-1 (SYNE1) as significantly elevated in LGSOC
253 tumors (Supplementary Table 8). Considering the importance of MUC16 in ovarian cancer disease
254 biology, we were motivated to investigate this protein alteration in LGSOC and HGSOC tissues
255 further.
256

257 **Mucin-16 (MUC16)/ cancer antigen 125 (CA125) is elevated and exhibits a predominantly**
258 **apical staining pattern in low versus high-grade serous ovarian cancers**

259 To further investigate elevation of MUC16 protein as a putatively conserved protein alteration in
260 LGSOC versus HGSOC tumors, we performed immunohistochemistry (IHC) analysis of tissues
261 for a subset of LGSOC (n=11) and HGSOC (n=24) tumors characterized within our discovery
262 cohort. A comparison of tumor cells stained positive for MUC16 between LGSOC and HGSOC
263 tumors showed HGSOC tumors overall have fewer MUC16-positive cells than LGSOC cells
264 (Figure 4B, Supplementary Table 10), a finding confirmed by three independent reviewers
265 (Cohen's kappa = 0.462, P < 1E-4, Supplementary Table 10). Further analysis of MUC16 staining
266 identified discrete localization patterns correlating within disease subtypes, where HGSOCs

267 exhibited a more membranous or combined apical and membranous staining pattern while
268 LGSOCs exhibited a predominantly apical staining pattern for MUC16 (Figure 4C). The increased
269 apical staining pattern in LGSOC tumors was also confirmed by three independent reviewers
270 (Fisher's Exact $P \leq 0.034$, Supplementary Table 10). We further include MUC16 IHC images for
271 a representative HGSOC case demonstrating apical and membranous staining, and an LGSOC case
272 exhibiting a predominant and intense apical membrane staining pattern (Figure 4D).
273

274 **Discussion**

275 Our deep proteomic analysis of benign fallopian tube tissues as well as low (LGSOC) and high
276 (HGSOC) grade serous ovarian cancers shows these samples can be stratified by variably abundant
277 protein alterations suggesting distinct proteome abundance profiles are characteristic of these
278 tissue types. Differential analysis of tumor (LGSOC and HGSOC) and benign fallopian tube tissue
279 identified that proteins elevated in fallopian tubes were largely enriched for pathways regulating
280 cilium development. Recent evidence from single cell studies has identified several subpopulations
281 of epithelial cell types exist within benign fallopian tube, including ciliated cell types[14,15]. This cell
282 population is considered to reflect a more differentiated subpopulation of fallopian tube epithelial
283 cells emerging from non-ciliated, secretory epithelial cell types[14,15]. The loss of proteins regulating
284 cilium development that we observe in LGSOC and HGSOC tissues is consistent with evidence
285 suggesting secretory epithelial cell types often exhibit greater neoplastic potential than other cell
286 types in fallopian tube epithelium[14]. We also find that proteins elevated in both LGSOC and
287 HGSOC tumors exhibit enrichment of pathways regulating protein translation, specifically
288 ribosome and translational elongation, as well as amino acid metabolism in comparison with
289 benign fallopian tube. Increased ribosome biogenesis and protein translation has been described

290 as a characteristic of ovarian cancer cells and as a possible therapeutic vulnerability in both
291 LGSOC and HGSOC[16,17]. Proteins uniquely elevated in HGSOC tumors compared to benign
292 fallopian tube were largely enriched for pathways regulating cell cycle and mitosis, which is
293 consistent with the high-grade phenotype of this disease[18]. Proteins uniquely elevated in LGSOC
294 were enriched for pathways regulating epithelial to mesenchymal transition including extracellular
295 matrix organization, beta1 integrin cell surface interactions, and hematopoietic cell-related
296 signaling, i.e. complement and coagulation. Beta1 integrin signaling has been implicated in
297 regulating migration of ovarian cancer cells in the context of interactions with extracellular matrix
298 proteins[19]. Our comparison with fallopian tube tissues has identified proteome alterations largely
299 consistent with the malignant phenotypes of LGSOC and HGSOC tumors in comparison to benign
300 fallopian tube.

301 Comparison of LGSOC and HGSOC revealed marked protein alterations between these
302 disease subtypes, including elevation of proteins correlating with proliferation and DNA
303 replication in HGSOC. We also observed elevation of diverse extracellular matrix proteins in
304 LGSOC tumors, including multiple collagen isoforms which is noteworthy considering the
305 enrichment of pathways regulating intercellular cell adhesion[20] we also observe in these tumors.
306 Recent global proteome analysis of tumors collected from women diagnosed with LGSOC or
307 HGSOC have been described by our team[6,9] and others[7], and we were motivated to compare
308 observed proteome alterations between LGSOC and HGSOC tumors from this study with these
309 independent cohorts to identify and validate proteome alterations that are highly conserved
310 between these disease subtypes. This comparison resulted in the identification of highly conserved
311 protein alterations exhibiting high quantitative correlation between LGSOC and HGSOC tumors
312 (Spearman Rho $\geq$ 0.82). These features demonstrated that proteins elevated in HGSOC tumors

313 correlate with enrichment of pathways regulating cell cycle and cell mitosis signaling, while those
314 elevated in LGSOC tumors correlated with pathways regulating intercellular adhesion and
315 defective cellular apoptosis. We also investigated putative drug targets exhibiting large differences
316 in abundance between LGSOC and HGSOC tumors and, among top targets, we identify cluster of
317 differentiation 73 (NT5E/CD73) as elevated in LGSOC versus HGSOC tumors. CD73 has been
318 shown to participate in an immune-related checkpoint pathway that promotes conversion of
319 exogenous adenosine triphosphate to adenosine by tumor cells which can suppress immune cell
320 function [21,22]. CD73 expression has been shown to correlate with poor disease outcome in HGSOC
321 and to be markedly elevated in HGSOC tumors that are enriched for a stromal-expression signature
322 also correlated with poor disease outcome[23]. Recent efforts investigating the feasibility to target
323 CD73 with a monoclonal antibody, i.e. Oleclumab, and the immune checkpoint inhibitor, i.e.
324 Durvalumab, in recurrent ovarian cancer have found this combination to be well tolerated[22].
325 LGSOC has been recently described as exhibiting an immunosuppressive tumor
326 microenvironment, particularly in the absence of mutations in the proto-oncogene B-Raf (BRAF)
327 or Kirsten rat sarcoma virus (KRAS)[24]. Our findings that CD73 is significantly elevated in LGSOC
328 versus HGSOC tumors warrants additional investigation of the role of this protein in regulating
329 the immune microenvironment of LGSOC tumors and will be the focus of future research.

330 Additional investigation of putatively conserved protein alterations between LGSOC and
331 HGSOC tumors identified mucin-16 (MUC16)/ cancer antigen 125 (CA125) as significantly
332 elevated in LGSOC versus HGSOC tumor tissues. MUC16 is a transmembrane glycoprotein that
333 is highly abundant in the female reproductive tract and can be actively shed from ovarian cancer
334 cells into blood plasma[8]. Circulating MUC16/ CA125 protein levels thus represents a measurable
335 biomarker that can assess evidence of disease and is a facet of routine diagnosis and disease

336 monitoring in the clinical management of ovarian cancer[3,8]. Comparison of the putative MUC16
337 interactome and highly conserved protein alterations observed between LGSOC and HGSOC
338 tumors identified nesprin-1 (SYNE1) as elevated in LGSOC tumors. SYNE1 and MUC16 have
339 been observed as commonly mutated gene targets in stomach cancer and tumors with mutations in
340 these genes have been shown to exhibit decreased immune cells as well as to correlate with lower
341 response to immunotherapy[25]. Shedding of MUC16 has been shown to occur as a product of
342 proteolytic cleavage of the carboxy-terminal ectodomain in the acidifying Golgi/ post-Golgi[26],
343 possibly by membrane-type 1 matrix metalloproteinase[27] followed by release of the N-terminal
344 CA125 region[27] into interstitial fluid and ultimately into circulating blood[8]. As we quantify
345 membrane-type 1 matrix metalloproteinase (MT1-MMP/ MMP-14/ P50281) protein in our
346 discovery cohort, we compared levels between LGSOC and HGSOC tumors, but we do not
347 observe this protein as significantly altered between these disease subtypes (MWU $p = 0.48$).
348 Recent evidence investigating mechanisms regulating cell surface retention of MUC16 have
349 implicated N-glycosylation mediated by N-acetylglucosaminyltransferase I (MGAT1) which has
350 been shown to promote increased retention of MUC16 at the cell surface[28]. This study further
351 identified that N-glycosylation of MUC16 promotes interaction with the protein galectin-3
352 (LGALS3) at the cell surface[28]. Notably, we identify LGALS3 as significantly elevated in LGSOC
353 versus HGSOC tumor tissues ($p<0.05$ across all cohorts assessed) and, although we quantify
354 MGAT1, we see this protein is significantly elevated in HGSOC tumors in our discovery cohort
355 (Supplementary Table 7), but we do not see this protein as significantly altered between LGSOC
356 versus HGSOC tissues in validation cohorts. If we consider this evidence in the context of our
357 findings, this suggests LGSOC tumor cells perhaps exhibit increased retention of MUC16 at the
358 cell surface. Circulating CA125 levels have been measured in both LGSOC and HGSOC patients,

359 although it has been noted that these levels are more commonly lower in LGSOC patients[3,29]. We
360 also find that circulating CA125 levels were lower in our LGSOC versus HGSOC patients (Table
361 1), providing further evidence in support of this hypothesis. A possible mechanism underlying
362 altered dynamics of MUC16 retention may be due to differential N-glycosylation of MUC16 in
363 LGSOC tumor cells, possibly due to altered enzymatic activity of MGAT1. Alternatively,
364 differences in MUC16 expression and shedding could relate to greater cleavage of the extracellular
365 domain in HGSOC, accounting for the greater shedding of CA125 and decreased membrane
366 expression. Future studies will investigate these hypotheses, including the comparison of cleaved
367 versus non-cleaved MUC16 levels in LGSOC and HGSOC tumors.

368 We also observe that LGSOC tumor cells exhibit a predominantly apical staining pattern
369 for MUC16 in comparison to HGSOC tumor cells. Similar findings were observed in murine
370 ovarian carcinomas where more intense apical expression of MUC16 was observed in grade 1
371 tumors[30]. Recent evidence has shown that MUC16 is maintained within apical membranes of
372 epithelial cells, such as in ocular epithelium[31], and to be dependent on glycosylation[28], which may
373 explain why we observe increased apical staining patterns for MUC16 in LGSOC tissues. Beyond
374 its role as a biomarker, MUC16 has been shown to promote cellular proliferation, invasion of
375 ovarian cancer cells[32], and has previously been shown to discourage immune surveillance, and to
376 be a potential target for immunotherapy[33]. Future efforts will focus on investigating mechanisms
377 of membrane retention of MUC16 in LGSOC and improving our understanding of how this
378 characteristic impacts LGSOC tumor cell biology.

379 Limitations for this study include small sample sizes for normal fallopian tube, LGSOC,
380 and HGSOC tissues in our discovery cohort. We aimed to address this limitation by prioritizing
381 protein alterations between LGSOC and HGSOC tumors that are also validated within global

382 proteomic data generated for independent cohorts of LGSOC and HGSOC patients. Another
383 limitation may be that samples were obtained by formalin-fixed, paraffin-embedded tissue instead
384 of fresh frozen tissue, however, comparison of fresh tissue samples and fixed frozen paraffin
385 embedded samples has not demonstrated differences in peptide identification and quantification[34].
386 Strengths of this study include the foundation provided for future proteomic research and the
387 contributions of our findings towards improving our understanding of molecular alterations
388 underlying ovarian cancer pathogenesis.
389

390 **Conclusion**

391 Our study contributes to our understanding of global proteome dynamics between normal fallopian
392 tube tissues, LGSOC, and HGSOC tumors, and provides insights into the relative abundance and
393 localization of conserved protein alterations between LGSOC and HGSOC, including CD73 and
394 the ovarian cancer biomarker MUC16/ CA125; these latter findings may also affect clinical
395 interpretation of circulating levels of MUC16/CA125 in these disease subtypes. Future study is
396 needed to determine the significance of protein alterations in the course of this disease, e.g. CD73
397 and the immune microenvironment of LGSOC tumors, which may serve as additional therapeutic
398 targets for disease treatment.
399

400 **Table 1: Patient and tumor clinicopathological characteristics**

Characteristic	High Grade Serous Ovarian Cancer (N = 24)	Low Grade Serous Ovarian Cancer (N = 12)	Benign Fallopian Tube (N = 12)
Mean age (range) –yr	58.1 (30-90)	52.0 (30-73)	45.2 (41-49)
Menopausal status – no. (%)			
Premenopausal	5 (20.8)	6 (50.0)	12 (100.0)
Postmenopausal	19 (79.2)	6 (50.0)	0 (0.0)
Mean BMI (range)	25.6 (22.5 – 30)	25.4 (20.7 – 30.8)	30.1 (19 – 44.1)
Race – no. (%)			
White	13 (54.2)	11 (91.7)	4 (33.3)
Black	7 (29.2)	0 (0.0)	4 (33.3)
Asian	4 (16.7)	1 (8.3)	2 (16.7)
Hispanic	0 (0.0)	0 (0.0)	2 (16.7)
FIGO stage – no. (%)			
I or II	2 (8.3)	3 (25.0)	-
IIIA	3 (12.5)	4 (33.3)	-
IIIB	6 (25.0)	1 (8.4)	-
IIIC	7 (29.2)	4 (33.3)	-
IV	6 (25.0)	0 (0.0)	-
Debulking			
RD0	12 (50.0)	7 (58.3)	-
RD1	9 (37.5)	4 (33.3)	-
Suboptimal	2 (8.3)	1 (8.4)	-
Unknown	1 (4.2)	0 (0.0)	-
Platinum Sensitivity – no (%)			
Sensitive	14 (58.3)	8 (66.6)	-
Resistant	4 (16.7)	1 (8.4)	-
Unknown	6 (25.0)	3 (25.0)	-
Mean CA125 (range)	4917.1 (329 – 50,000)	672.7 (70 – 1576)	-

401

402

403

404 **Data Availability**

405 Proteomic data generated in this study is accessible at the ProteomeXChange under accession
406 PXD050642.

407 **Author Contributions**

408 C.M.T., N.W.B., T.P.C. lead the study. C.M.T, P.F., J.O., G.L.M. performed identification of
409 clinical specimens, C.M.T., G.L.M., K.M.D performed clinical data analysis. K.A.C., J.O., and
410 C.M.T. performed sample collections and molecular extraction. N.W.B., J.O., T.A., B.L.H,
411 generated and analyzed proteomics data. P.M.F. P.A.B, S.M.L performed pathology review.
412 C.M.T., N.W.B., wrote the manuscript, P.M.F., J.O., T.A., B.L.H, K.R., K.K.W, D.G., S.L.,
413 A.K.S., R.C.B, K.M.D., N.T.P, G.L.M, T.P.C reviewed the manuscript. All authors reviewed and
414 approved the final manuscript.

415 **Declaration of Interests**

416 Nothing to disclose.

417 **Acknowledgements**

418 Funding for this project was provided from the Uniformed Services University of the Health
419 Sciences from the Defense Health Program to the Henry M Jackson Foundation (HJF) for the
420 Advancement of Military Medicine Inc. Gynecologic Cancer Center of Excellence Program,
421 including awards HU0001-20-2-0033, HU0001-21-2-0027, HU0001-22-2-0016, and HU0001-23-
422 2-0038 (PI: Neil T Phippen, Co-PI: G. Larry Maxwell).

423

424

425 **Disclaimer**

426 The views expressed herein are those of the authors and do not reflect the official policy of the
427 Uniformed Services University of the Health Sciences, the Henry M. Jackson Foundation for the
428 Advancement of Military Medicine, Inc., Inova Health System, the Department of Army/Navy/Air
429 Force, Department of Defense, or U.S. Government. Mention of trade names, commercial
430 products, or organizations does not imply endorsement by the U.S. Government.

431

432

433 **References**

434 1 Torre, L. A. *et al.* Ovarian cancer statistics, 2018. *CA Cancer J Clin* **68**, 284-296,
435 doi:10.3322/caac.21456 (2018).
436 2 Siegel, R. L., Giaquinto, A. N. & Jemal, A. Cancer statistics, 2024. *CA Cancer J Clin* **74**,
437 12-49, doi:10.3322/caac.21820 (2024).
438 3 Slomovitz, B. *et al.* Low-grade serous ovarian cancer: State of the science. *Gynecol*
439 *Oncol* **156**, 715-725, doi:10.1016/j.ygyno.2019.12.033 (2020).
440 4 Zarei, S. *et al.* Clinicopathologic, Immunohistochemical, and Molecular Characteristics
441 of Ovarian Serous Carcinoma With Mixed Morphologic Features of High-grade and
442 Low-grade Serous Carcinoma. *Am J Surg Pathol* **44**, 316-328,
443 doi:10.1097/PAS.0000000000001419 (2020).
444 5 Gershenson, D. M. *et al.* Trametinib versus standard of care in patients with recurrent
445 low-grade serous ovarian cancer (GOG 281/LOGS): an international, randomised, open-
446 label, multicentre, phase 2/3 trial. *Lancet* **399**, 541-553, doi:10.1016/S0140-
447 6736(21)02175-9 (2022).
448 6 Wong, K. K. *et al.* Integrated multi-omic analysis of low-grade ovarian serous carcinoma
449 collected from short and long-term survivors. *J Transl Med* **20**, 606, doi:10.1186/s12967-
450 022-03820-x (2022).
451 7 Vallejos, R. *et al.* Changes in the tumour microenvironment mark the transition from
452 serous borderline tumour to low-grade serous carcinoma. *J Pathol*,
453 doi:10.1002/path.6338 (2024).
454 8 Giamougiannis, P., Martin-Hirsch, P. L. & Martin, F. L. The evolving role of MUC16
455 (CA125) in the transformation of ovarian cells and the progression of neoplasia.
456 *Carcinogenesis* **42**, 327-343, doi:10.1093/carcin/bgab010 (2021).
457 9 Lee, S. *et al.* Molecular Analysis of Clinically Defined Subsets of High-Grade Serous
458 Ovarian Cancer. *Cell Rep* **31**, 107502, doi:10.1016/j.celrep.2020.03.066 (2020).
459 10 Burdett, N. L. *et al.* Multiomic analysis of homologous recombination-deficient end-stage
460 high-grade serous ovarian cancer. *Nat Genet* **55**, 437-450, doi:10.1038/s41588-023-
461 01320-2 (2023).
462 11 Ritchie, M. E. *et al.* limma powers differential expression analyses for RNA-sequencing
463 and microarray studies. *Nucleic Acids Res* **43**, e47, doi:10.1093/nar/gkv007 (2015).
464 12 Subramanian, A. *et al.* Gene set enrichment analysis: a knowledge-based approach for
465 interpreting genome-wide expression profiles. *Proc Natl Acad Sci U S A* **102**, 15545-
466 15550, doi:10.1073/pnas.0506580102 (2005).
467 13 Tang, D. *et al.* SRplot: A free online platform for data visualization and graphing. *PLoS*
468 *One* **18**, e0294236, doi:10.1371/journal.pone.0294236 (2023).
469 14 Dinh, H. Q. *et al.* Single-cell transcriptomics identifies gene expression networks driving
470 differentiation and tumorigenesis in the human fallopian tube. *Cell Rep* **35**, 108978,
471 doi:10.1016/j.celrep.2021.108978 (2021).
472 15 Ghosh, A., Syed, S. M. & Tanwar, P. S. In vivo genetic cell lineage tracing reveals that
473 oviductal secretory cells self-renew and give rise to ciliated cells. *Development* **144**,
474 3031-3041, doi:10.1242/dev.149989 (2017).
475 16 Yan, S. *et al.* The Potential of Targeting Ribosome Biogenesis in High-Grade Serous
476 Ovarian Cancer. *Int J Mol Sci* **18**, doi:10.3390/ijms18010210 (2017).

17 Kang, J. *et al.* Ribosomal proteins and human diseases: molecular mechanisms and targeted therapy. *Signal Transduct Target Ther* **6**, 323, doi:10.1038/s41392-021-00728-8 (2021).
18 Lopez-Reig, R. & Lopez-Guerrero, J. A. The hallmarks of ovarian cancer: proliferation and cell growth. *EJC Suppl* **15**, 27-37, doi:10.1016/j.ejcsup.2019.12.001 (2020).
19 Casey, R. C. & Skubitz, A. P. CD44 and beta1 integrins mediate ovarian carcinoma cell migration toward extracellular matrix proteins. *Clin Exp Metastasis* **18**, 67-75, doi:10.1023/a:1026519016213 (2000).
20 Yi, B. R., Kim, T. H., Kim, Y. S. & Choi, K. C. Alteration of epithelial-mesenchymal transition markers in human normal ovaries and neoplastic ovarian cancers. *Int J Oncol* **46**, 272-280, doi:10.3892/ijo.2014.2695 (2015).
21 Ploeg, E. M. *et al.* A Novel Bispecific Antibody for EpCAM-Directed Inhibition of the CD73/Adenosine Immune Checkpoint in Ovarian Cancer. *Cancers (Basel)* **15**, doi:10.3390/cancers15143651 (2023).
22 Mirza, M. R. *et al.* NSGO-OV-UMB1/ENGOT-OV30: A phase II study of durvalumab in combination with the anti-CD73 monoclonal antibody Oleclumab in patients with relapsed ovarian cancer. *Gynecol Oncol* **188**, 103-110, doi:10.1016/j.ygyno.2024.06.017 (2024).
23 Turcotte, M. *et al.* CD73 is associated with poor prognosis in high-grade serous ovarian cancer. *Cancer Res* **75**, 4494-4503, doi:10.1158/0008-5472.CAN-14-3569 (2015).
24 Wong, K.-K. & Gershenson, D. M. Abstract 135: Immunosuppressive microenvironment in low-grade serous ovarian carcinoma. *Cancer Research* **78**, 135-135, doi:10.1158/1538-7445.am2018-135 (2018).
25 Yue, T. *et al.* Two Similar Signatures for Predicting the Prognosis and Immunotherapy Efficacy of Stomach Adenocarcinoma Patients. *Front Cell Dev Biol* **9**, 704242, doi:10.3389/fcell.2021.704242 (2021).
26 Das, S. *et al.* Membrane proximal ectodomain cleavage of MUC16 occurs in the acidifying Golgi/post-Golgi compartments. *Sci Rep* **5**, 9759, doi:10.1038/srep09759 (2015).
27 Bruney, L., Conley, K. C., Moss, N. M., Liu, Y. & Stack, M. S. Membrane-type I matrix metalloproteinase-dependent ectodomain shedding of mucin16/ CA-125 on ovarian cancer cells modulates adhesion and invasion of peritoneal mesothelium. *Biol Chem* **395**, 1221-1231, doi:10.1515/hsz-2014-0155 (2014).
28 Taniguchi, T. *et al.* N-Glycosylation affects the stability and barrier function of the MUC16 mucin. *J Biol Chem* **292**, 11079-11090, doi:10.1074/jbc.M116.770123 (2017).
29 But, I. & Gorisek, B. Preoperative value of CA 125 as a reflection of tumor grade in epithelial ovarian cancer. *Gynecol Oncol* **63**, 166-172, doi:10.1006/gyno.1996.0301 (1996).
30 Wang, Y. *et al.* MUC16 expression during embryogenesis, in adult tissues, and ovarian cancer in the mouse. *Differentiation* **76**, 1081-1092, doi:10.1111/j.1432-0436.2008.00295.x (2008).
31 Mantelli, F. & Argueso, P. Functions of ocular surface mucins in health and disease. *Curr Opin Allergy Clin Immunol* **8**, 477-483, doi:10.1097/ACI.0b013e32830e6b04 (2008).
32 Felder, M. *et al.* MUC16 (CA125): tumor biomarker to cancer therapy, a work in progress. *Mol Cancer* **13**, 129, doi:10.1186/1476-4598-13-129 (2014).

522 33 Zhai, Y. *et al.* MUC16 affects the biological functions of ovarian cancer cells and induces
523 an antitumor immune response by activating dendritic cells. *Ann Transl Med* **8**, 1494,
524 doi:10.21037/atm-20-6388 (2020).
525 34 Bateman, N. W. & Conrads, T. P. Recent advances and opportunities in proteomic
526 analyses of tumour heterogeneity. *J Pathol* **244**, 628-637, doi:10.1002/path.5036 (2018).

527

528

529 **Figure Legends**

530 **Figure 1: Workflow supporting quantitative proteomic analyses and validation of proteome**
531 **alterations in low (LGSOC) and high-grade (HGSOC) serous ovarian cancers.** Whole tissue
532 collections from benign fallopian tube, LGSOC, and HGSOC tissues were performed using laser
533 microdissection. Tissue collections underwent multiplexed, quantitative proteomic analysis using
534 isobaric tagging, i.e. tandem mass tags (TMT-11), followed by liquid chromatography, tandem
535 mass spectrometry (LC-MS/MS) analysis on an Orbitrap mass spectrometer. Proteome alterations
536 identified in discovery cohorts of LGSOC and HGSOC tissues were validated using global
537 proteome data for independent cohorts of LGSOC (n=25) and HGSOC (n=49) tumors[6,7,9] and
538 included the finding that mucin-16 (MUC16) is elevated in LGSOC tumors which was further
539 verified by immunohistochemistry analysis of LGSOC and HGSOC tissues by three independent
540 reviewers.

541

542 **Figure 2: Differential proteomic analysis of whole tissue collections from normal fallopian**
543 **tube with low (LGSOC) and high-grade (HGSOC) serous ovarian cancers.** A: Principal
544 component analysis (PCA) of the top 500 most variably abundant proteins quantified across
545 samples; proteins prioritized based on median absolute deviation. B: Comparison of proteins
546 significantly altered between HGSOC or LGSOC and benign fallopian tube collections; proteins
547 reflect LIMMA adjusted p-value < 0.05, fold-change $\pm$ 2.0. C: Pathway analysis of proteins co-
548 altered between HGSOC and LGSOC vs benign fallopian tube collections; top hallmark and
549 canonical pathways (gsea-msigdb.org) enriched among proteins elevated (84) or decreased (457)
550 in HGSOC and LGSOC versus benign fallopian tube collections. D: Pathway analysis of proteins
551 uniquely elevated in HGSOC or LGSOC vs normal fallopian tube collections; top hallmark and

552 canonical pathways (gsea-msigdb.org) enriched among proteins elevated in HGSOC (300) or
553 LGSOC (158) tumors versus benign fallopian tube collections.

554

555 **Figure 3: Differential proteomic analysis of low (LGSOC) and high-grade (HGSOC) serous**
556 **ovarian cancers and validation of proteome alterations in independent LGSOC and HGSOC**
557 **cohorts.** A: Workflow for the prioritization of conserved protein alterations between LGSOC and
558 HGSOC tumors in discovery and validation cohorts[6,7,9]. B: Volcano plot reflects proteins
559 significantly altered between LGSOC and HGSOC tumors in discovery cohort; proteins reflect
560 LIMMA adjusted p-value < 0.05, fold-change ± 1.5. C: Proteins co-altered between LGSOC and
561 HGSOC tumors in discovery and validation cohorts; 275 co-altered proteins passing an adjusted
562 p-value < 0.05. D: Pathway analysis of proteins co-altered between LGSOC and HGSOC tumors
563 in discovery and validation cohorts; top hallmark and canonical pathways (gsea-msigdb.org)
564 enriched among proteins elevated (93) or decreased (180) between LGSOC and HGSOC tumors.

565

566 **Figure 4: Immunohistochemical analysis of Mucin-16 (MUC16) in low (LGSOC) and high-**
567 **grade (HGSOC) serous ovarian cancers.** A: Mucin-16 (MUC16) protein abundance in LGSOC
568 and HGSOC tumors from discovery or validation A cohorts; * = LIMMA adjusted p-value < 0.05,
569 **** = LIMMA adjusted p-value < 1E-4. MUC16 was significantly elevated in LGSOC tumors
570 in Validation B cohort, adjusted p-value= 0.052 (not shown). B: Comparison of cells stained
571 positive for MUC16 following immunohistochemical analysis of LGSOC (n=10) and HGSOC
572 (n=24) tissues; data and p-value reflects Mann Whitney Rank Sum testing comparing "PATH1"
573 reviews (Supplementary Table 10). MUC16 confirmed elevated in LGSOC tumors by three

574 independent reviewers (Cohen's kappa = 0.462, P < 1E-4, Supplementary Table 10). C:
575 Comparison of MUC16 staining patterns in LGSOC (n=10) and HGSOC (n=24) tissues identified
576 by "PATH1"; tumor cell populations were identified to exhibit predominantly apical or apical-
577 membranous MUC16 staining and predominantly apical staining in LGSOC tumors was
578 confirmed by three independent reviewers (Fisher's Exact P ≤ 0.034, Supplementary Table 10).
579 D: MUC16 immunohistochemistry stains in tissue sections from one representative LGSOC and
580 HGSOC patient tumor.

581 **Supplementary Tables**

582 1) Supplementary Table 1 (S1): Discovery cohort details
583 2) Supplementary Table 2 (S2): Global proteome matrix
584 3) Supplementary Table 3 (S3): Differential analysis of LGSOC vs Fallopian Tube
585 4) Supplementary Table 4 (S4): Differential analysis of HGSOC vs Fallopian Tube
586 5) Supplementary Table 5 (S5): Pathway analysis of proteins co-altered between HGSOC and
587 LGSOC vs Fallopian Tube.
588 6) Supplementary Table 6 (S6): Pathway analysis of proteins uniquely elevated in HGSOC or
589 LGSOC tumors vs Fallopian Tube.
590 7) Supplementary Table 7 (S7): Differential analysis of LGSOC vs HGSOC
591 8) Supplementary Table 8 (S8): Proteins significantly co-altered in LGSOC vs HGSOC between
592 Discovery and Validation A & B cohorts.
593 9) Supplementary Table 9 (S9): Pathway analysis of proteins significantly co-altered between
594 HGSOC and LGSOC tumors in Discovery and Validation A & B cohorts.
595 10) Supplementary Table 10 (S10): MUC16 immunohistochemistry analysis detailing expert
596 pathology reviews from three independent reviewers, i.e. PATH1, PATH2 and PATH3.

Figure1

Normal Fallopian Tube, Low (LGSOC) & High-Grade (HGSOC) Serous Ovarian Cancer

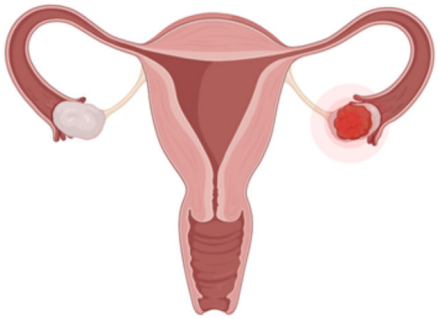

Collection of Tissues by Laser Microdissection Followed by Quantitative Proteomics

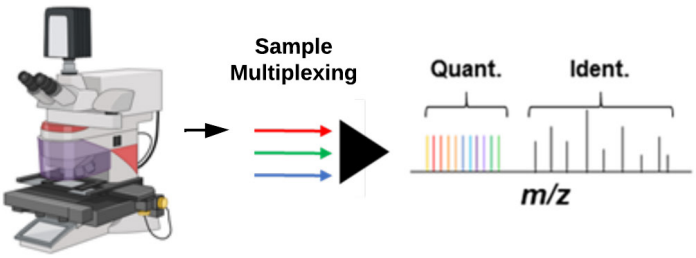

Conserved Proteome Alterations in LGSOC & HGSOC Tissues

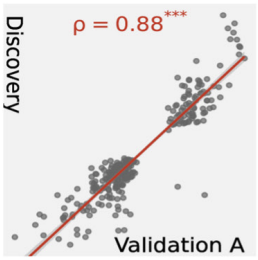

	LGSOC	HGSOC
Discovery	12	24
Validation A: Wong KK (2022) & Lee S (2020)	14	30
Validation B: Vallejos R (2024)	11	19
TOTAL	37	73

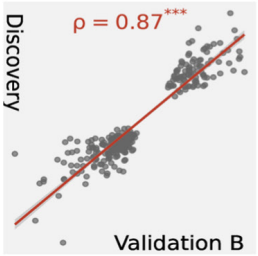

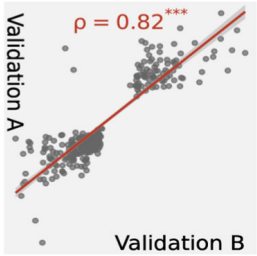

LGSOC

MUC-16 IHC

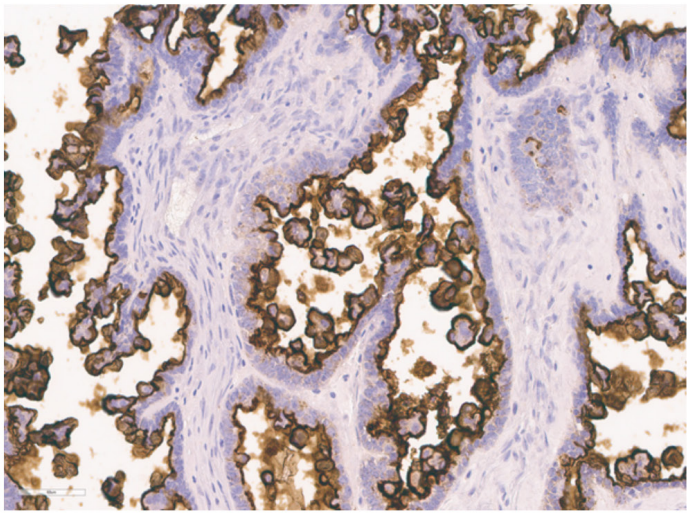

Figure 2

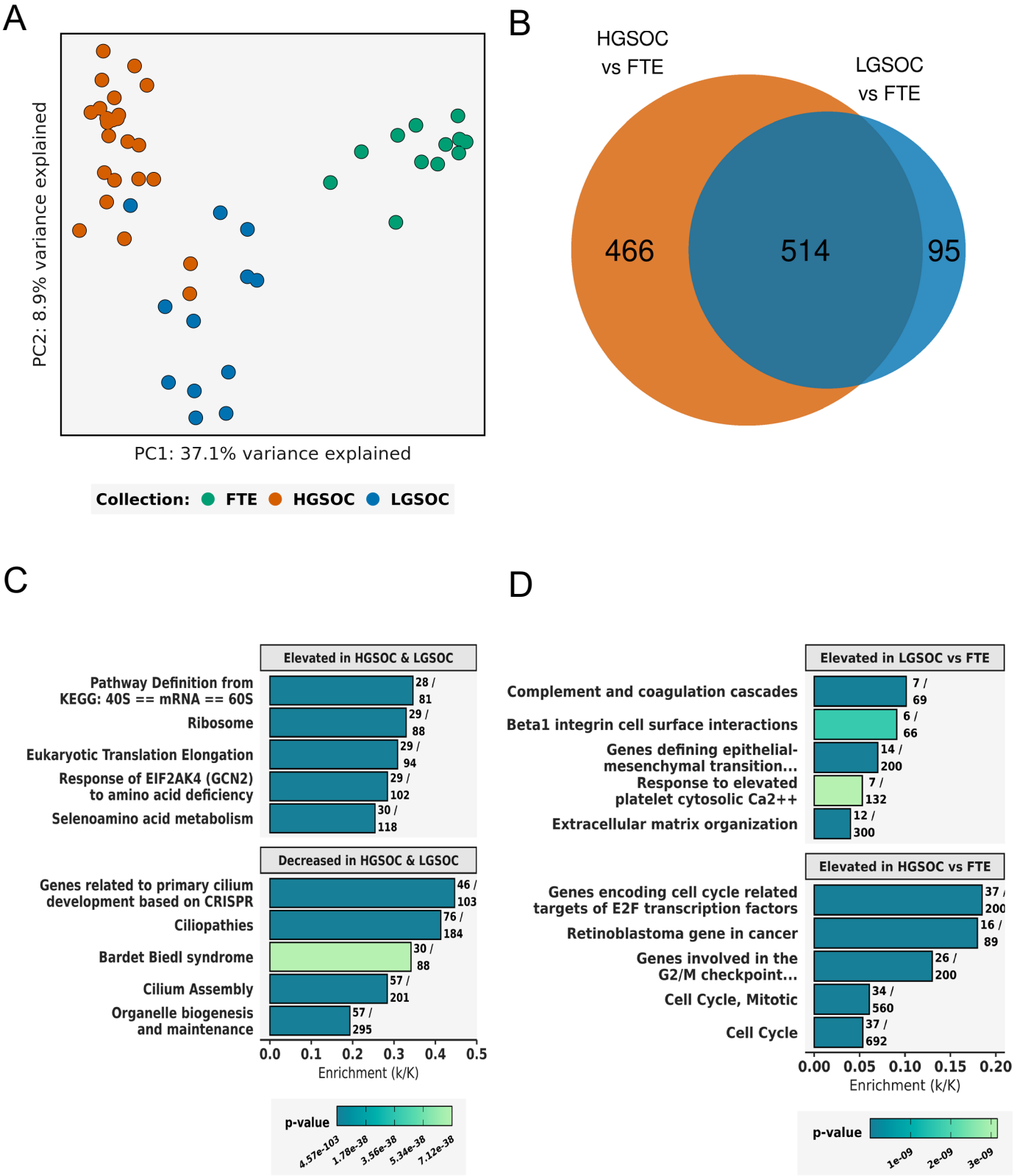
A
PC2: 8.9% variance explained
PC1: 37.1% variance explained
Collection: FTE HGSOC LGSOC
B
HGSOC vs FTE
LGSOC vs FTE
466
514
95
C
Elevated in HGSOC & LGSOC
Pathway Definition from KEGG: 40S == mRNA == 60S
28 / 81
Ribosome
29 / 88
Eukaryotic Translation Elongation
29 / 94
Response of EIF2AK4 (GCN2) to amino acid deficiency
29 / 102
Selenoamino acid metabolism
30 / 118
Decreased in HGSOC & LGSOC
Genes related to primary cilium development based on CRISPR
46 / 103
Ciliopathies
76 / 184
Bardet Biedl syndrome
30 / 88
Cilium Assembly
57 / 201
Organelle biogenesis and maintenance
57 / 295
0.0 0.1 0.2 0.3 0.4 0.5
Enrichment (k/K)
p-value
4.57e-103 1.78e-38 3.56e-38 5.34e-38 7.12e-38
D
Elevated in LGSOC vs FTE
Complement and coagulation cascades
7 / 69
Beta1 integrin cell surface interactions
6 / 66
Genes defining epithelial-mesenchymal transition...
14 / 200
Response to elevated platelet cytosolic Ca2++
7 / 132
Extracellular matrix organization
12 / 300
Elevated in HGSOC vs FTE
Genes encoding cell cycle related targets of E2F transcription factors
37 / 200
Retinoblastoma gene in cancer
16 / 89
Genes involved in the G2/M checkpoint...
26 / 200
Cell Cycle, Mitotic
34 / 560
Cell Cycle
37 / 692
0.00 0.05 0.10 0.15 0.20
Enrichment (k/K)
p-value
1e-09 2e-09 3e-09

Figure 3

A

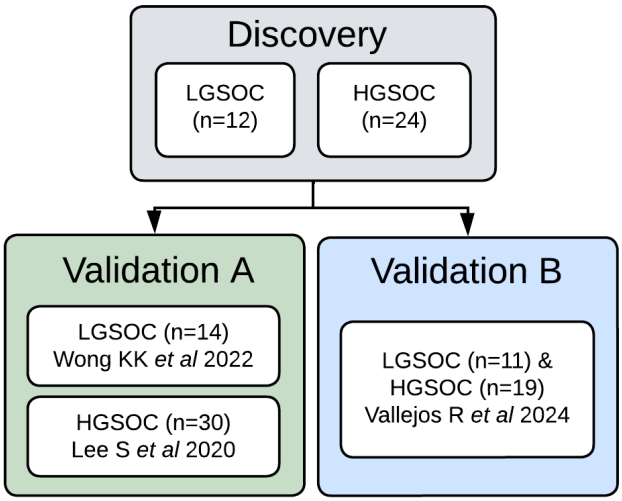

B

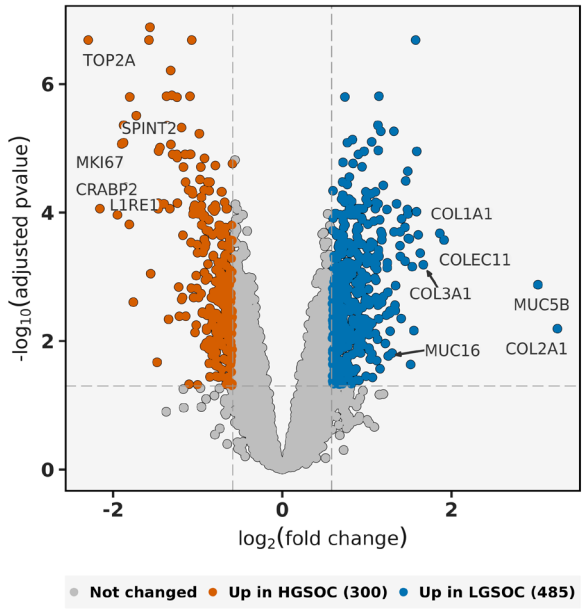

C

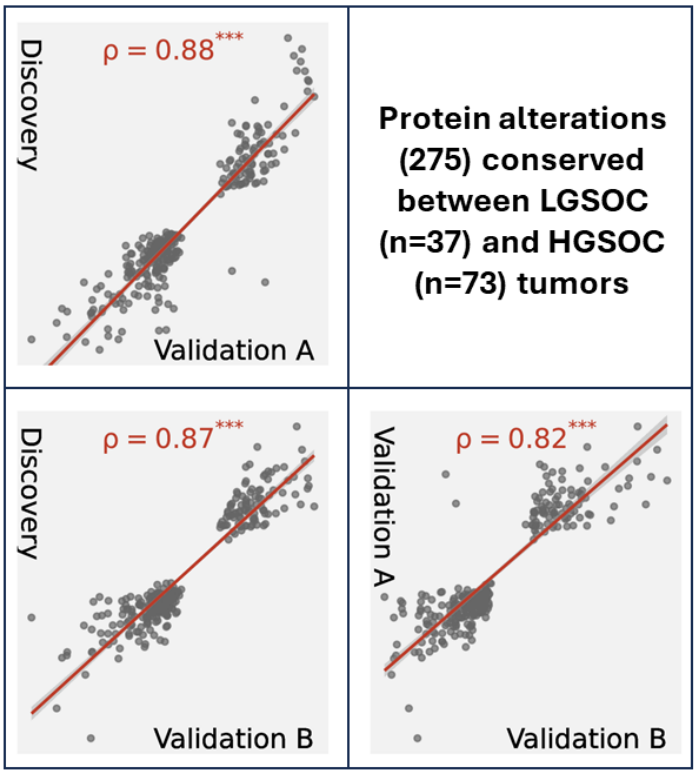

D

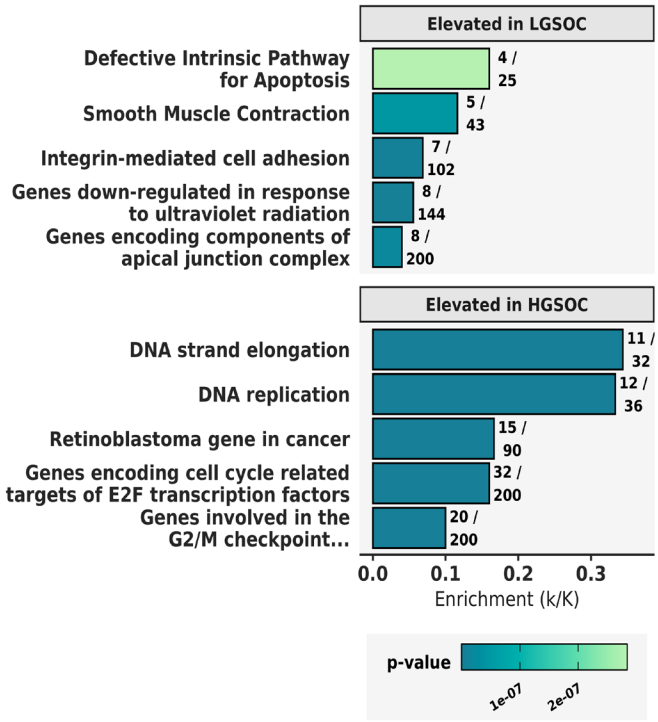

Figure 4

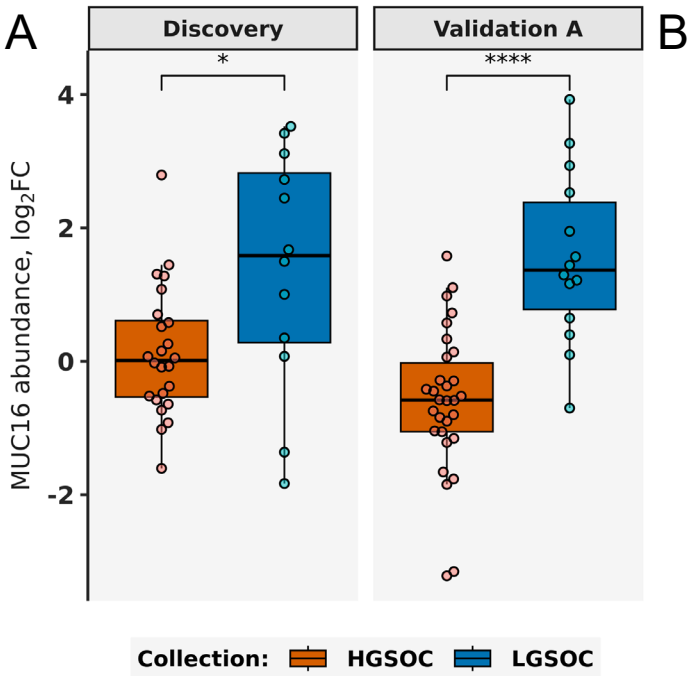
A
Discovery
Validation A
*
****
MUC16 abundance, log2FC
4
2
0
-2
Collection:
HGSOC
LGSOC

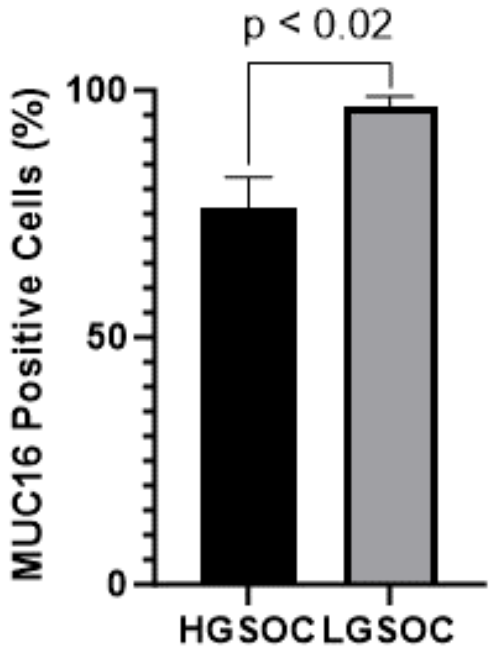
B
p < 0.02
MUC16 Positive Cells (%)
100
50
0
HGSOC
LGSOC

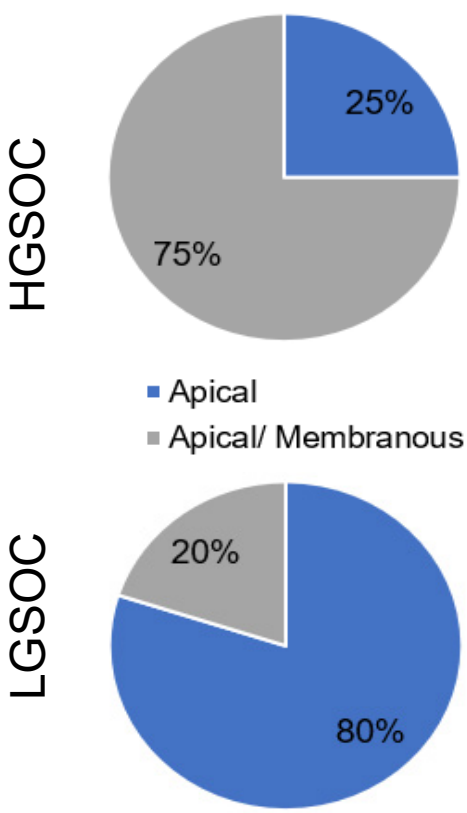
C
HGSOC
25%
75%
Apical
Apical/ Membranous
LGSOC
20%
80%

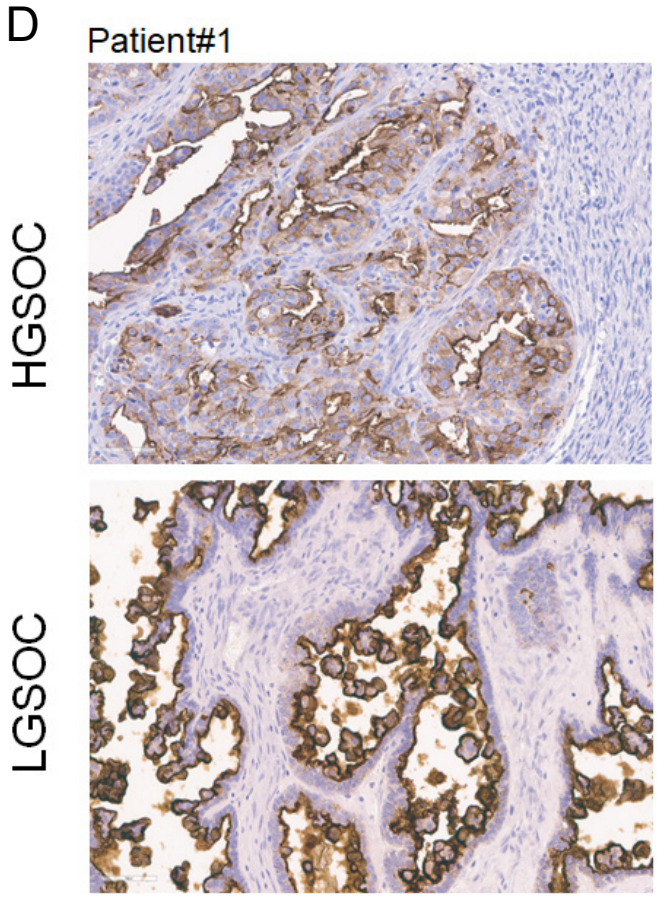
D
Patient#1
HGSOC
LGSOC